ResearchGate

See discussions, stats, and author profiles for this publication at:
https://www.researchgate.net/publication/321750757

Cryptic diversity in the Oecomys roberti complex: Revalidation of Oecomys tapajinus (Rodentia, Cricetidae)

Article *in* Journal of Mammalogy · December 2017

DOI: 10.1093/jmammal/gyx149

CITATIONS
0

READS
104

8 authors, including:

Rita Gomes Rocha
Universidade Federal do Espírito Santo
47 PUBLICATIONS **169** CITATIONS

SEE PROFILE

Rafaela Duda
Universidade Federal do Espírito Santo
6 PUBLICATIONS **20** CITATIONS

SEE PROFILE

Iracilda Sampaio
Federal University of Pará
541 PUBLICATIONS **3,922** CITATIONS

SEE PROFILE

Yuri Luiz Reis Leite
Universidade Federal do Espírito Santo
181 PUBLICATIONS **1,495** CITATIONS

SEE PROFILE

Some of the authors of this publication are also working on these related projects:

Origin and diversification of the genus Nectomys Peters, 1861 (Cricetidae: Sigmodontinae) View project

Dendrogene project View project

All content following this page was uploaded by Yuri Luiz Reis Leite on 12 December 2017.

The user has requested enhancement of the downloaded file.

Journal of Mammalogy, xx(x):1–13, 2017
DOI:10.1093/jmammal/gyx149

Cryptic diversity in the *Oecomys roberti* complex: revalidation of *Oecomys tapajinus* (Rodentia, Cricetidae)

Rita G. Rocha,* Rafaela Duda, Tamara Flores, Rogério Rossi, Iracilda Sampaio, Ana C. Mendes-Oliveira, Yuri L. R. Leite, and Leonora P. Costa

Departamento de Ciências Biológicas, Centro de Ciências Humanas e Naturais, Universidade Federal do Espírito Santo, 29075-910 Vitória, Espírito Santo, Brasil (RGR, RD, YLRL, LPC)
Mastozoologia—PPGZOOL, Coordenação de Zoologia, Museu Paraense Emílio Goeldi, 66077-530 Belém, Pará, Brasil (TF)
Instituto de Biociências, Universidade Federal de Mato Grosso, Av. Fernando Correa da Costa, 2367, 78060-900 Cuiabá, Mato Grosso, Brasil (RR)
Laboratório de Genética e Biologia Molecular, Instituto de Estudos Costeiros, Universidade Federal do Pará, Campus Universitário de Bragança, 68600-000 Bragança, Pará, Brasil (IS)
Laboratório de Ecologia e Zoologia de Vertebrados – Mastozoologia, Instituto de Ciências Biológicas, Universidade Federal do Pará, 66077-530 Belém, Pará, Brasil (ACM-O)

* *Correspondent: ritagomesrocha@gmail.com*

Oecomys tapajinus (Tapajós Oecomys) is currently a junior synonym of *Oecomys roberti* (Robert's Oecomys), a widely distributed Amazonian mouse, which probably represents a complex of cryptic species. We investigated the taxonomic status of *O. tapajinus* by integrating phylogenetic analyses of DNA sequences and morphological analyses of museum specimens. We were able to confirm that *O. tapajinus* is a valid species from eastern Amazonia and the transition to the Brazilian Cerrado, where it is sympatric with *O. roberti*. *Oecomys tapajinus* is characterized by a unique combination of morphological traits, high morphological variation, and genetic differentiation and structure related to the complex system of the Amazon River. Potential additional entities within the *O. roberti* complex emerged from our analyses, and further investigation with larger series may shed light on the taxonomic status of this species complex.

Oecomys tapajinus (rato-da-árvore do Tapajós) é atualmente considerado um sinónimo júnior de *Oecomys roberti* (rato-da-árvore de Robert), um roedor amplamente distribuído na Amazônia, e que provavelmente representa um complexo de espécies crípticas. Neste trabalho investigamos o status taxonômico de *O. tapajinus*, integrando análises filogenéticas de sequências de ADN e análises morfológicas de espécimes de museus. Confirmamos o status de *O. tapajinus* como uma espécie válida que ocorre no este da Amazônia e na transição com o Cerrado Brasileiro, onde é simpátrico com *O. roberti*. *Oecomys tapajinus* é caracterizado por uma combinação única de caracteres morfológicos, uma alta variação morfológica, e uma diferenciação e estrutura genética associada ao sistema complexo do Rio Amazonas. Este trabalho também revelou outras potenciais unidades dentro do complexo *O. roberti* que merecem investigação adicional com maiores séries amostrais e que irão ajudar a clarificar o status taxonômico deste complexo de espécies.

Key words: Amazonia, *Oecomys*, Oryzomyini, Sigmodontinae, species limits, systematics, taxonomy

Originally described as a subgenus of *Oryzomys* (rice rats) by Thomas (1906), the taxonomic breadth and definition of *Oecomys* has been contentious. Hershkovitz (1960) revised *Oryzomys* (*Oecomys*) and merged 25 species into only 2, thus severely underestimating its diversity (e.g., Patton et al. 2000; Voss et al. 2001). Recent studies treated *Oecomys* as generic level and confirmed its monophyletic status within Oryzomyini genera (Smith and Patton 1999; Weksler 2003, 2006). Currently, *Oecomys* is one of the most diverse genera of Oryzomyini, comprising 17 species (Carleton and Musser 2015; Pardiñas

© 2017 American Society of Mammalogists, www.mammalogy.org

Downloaded from https://academic.oup.com/jmammal/advance-article-abstract/doi/10.1093/jmammal/gyx149/4697216
by Universidade Federal do Espírito Santo user
on 11 December 2017

et al. 2016). In addition, there are 29 attributed synonyms, some of which may represent valid taxa, and several species with questionable taxonomic status (Rosa et al. 2012; Carleton and Musser 2015). New species continue to be described (e.g., Carleton et al. 2009; Pardiñas et al. 2016), and only continued faunal surveys and further taxonomic research will enhance our understanding of the diversity in the genus *Oecomys* (Carleton and Musser 2015).

As currently understood, Robert's Oecomys (*Oecomys roberti* Thomas 1904) is broadly distributed in Amazonia (Brazil, Bolivia, Colombia, Guyana, Peru, Surinam, and Venezuela), and was provisionally treated as monotypic (Carleton and Musser 2015). However, it may well represent a complex of cryptic species (Rocha et al. 2015). Two synonyms were recognized: *Oecomys tapajinus* (Thomas 1909), known from the east bank of the Tapajós River, Pará, Brazil; and *Oecomys guianae* (Thomas 1910), the Guianan Oecomys, known from the Supinaam River, Demerara-Mahaica, Guyana (Carleton and Musser 2015). Sampling gaps, mainly in eastern and northern Amazonia, add an additional challenge to our understanding of these taxonomic entities.

During an 18-month inventory of small mammals in the Amazonia-Cerrado ecotone in the mid-Araguaia River, central Brazil, we collected several unidentified specimens of *Oecomys*. Phylogenetic analyses of mitochondrial DNA sequences revealed that they comprised a monophyletic cluster of specimens exhibiting high levels of intrapopulational morphological variation. Although these specimens had been previously allied to Cleber's Oecomys (*Oecomys cleberi* Locks 1981—Rocha et al. 2011a), further analyses revealed they represented different species (Rocha et al. 2012). The specimens from the Araguaia River were then associated to either *O. roberti* proper, or treated as *Oecomys* gr. *roberti* in Rocha et al. (2015), due to their reciprocally monophyletic relationship and relatively high genetic distance separating these 2 forms (Rocha et al. 2011a, 2015).

Short of a full taxonomic revision of the genus *Oecomys*, we feel that the best approach is to compare our voucher specimens with type material for proper identification (e.g., Voss et al. 2001; Carleton et al. 2009). Moreover, molecular phylogenies and morphological data have been combined to solve taxonomic problems (e.g., Rosa et al. 2012; Pardiñas et al. 2016). Specifically, DNA sequences from type specimens, or genetypes (Chakrabarty 2010), are helpful when dealing with poorly known genera like *Oecomys* (Rocha et al. 2012), where species limits and geographic variation are still unclear.

Considering that cryptic species are those that "are, or have been, classified as a single nominal species because they are at least superficially morphologically indistinguishable" (Bickford et al. 2006:149), we aimed to elucidate the cryptic diversity in the *O. roberti* complex by integrating molecular and morphological analyses of specimens collected throughout the Amazon basin (Brazil and Guyana). We compared DNA sequences from topotypes of *O. roberti* and *O. tapajinus*, and external and cranial morphology of museum specimens, including all type specimens of the *O. roberti* complex, in order to investigate differences among putative taxonomic entities. We were able to revalidate *O. tapajinus* and refine its morphological diagnosis and geographic distribution. We also explored the spatial distribution of the genetic diversity within this species to understand current and historical factors responsible for such diversity.

Materials and Methods

Data sampling and specimen identification.—Specimens and tissue samples belonging to the *O. roberti* complex, including its 2 putative synonyms *O. tapajinus* and *O. guianae*, were obtained from localities in eastern and northern Amazonia (Fig. 1; Supplementary Data SD1 and SD2). All parts of the study involving live animals followed the guidelines of the American Society of Mammalogists (Sikes et al. 2016). To associate each specimen with a taxon name, we used a combination of molecular and geographic criteria from previous studies (Patton et al. 2000; Rocha et al. 2011a, 2012, 2015). *Oecomys roberti* is a well-defined cluster of specimens, including its topotype. Previously unidentified specimens collected in the Araguaia, Xingu, and Tapajós rivers (Rocha et al. 2011a, 2015) also form a monophyletic clade, and we tentatively named them *O. tapajinus*, to test if they comprise a valid species. For the 2 sets of specimens to which we were unable to assign a specific epithet due to the lack of previous phylogenetic analysis, we added geographical designations, namely *O. roberti* Guyana and *O. roberti* Juruá. Specimen vouchers and tissues used in this study are housed in the following institutions: BMNH, The Natural History Museum (London, United Kingdom); MBML, Museu de Biologia Professor Mello Leitão (Santa Teresa, Brazil); MPEG, Museu Paraense Emílio Goeldi (Belém, Brazil); MVZ, Museum of Vertebrate Zoology (Berkeley, California, United States); MZUSP, Museu de Zoologia da Universidade de São Paulo (São Paulo, Brazil); UFES-MAM, Coleção de Mamíferos da Universidade Federal do Espírito Santo (Vitória, Espírito Santo, Brazil); UFES-CTA, Coleção de Tecidos Animais da Universidade Federal do Espírito Santo (Vitória, Espírito Santo, Brazil); UFMG, Coleção de Mamíferos da Universidade Federal de Minas Gerais (Belo Horizonte, Minas Gerais, Brazil); UFPAM, Coleção de Mamíferos da Universidade Federal do Pará (Belém, Pará, Brazil).

Morphological data and morphometric analyses.—We examined 83 specimens (skins and skulls) of the *O. roberti* complex (*O. roberti* Guyana $n = 10$, *O. roberti* $n = 15$, *O. tapajinus* $n = 58$; see Supplementary Data SD1 for a list of specimens examined). Morphological characters were described and compared following Weksler (2006) and Carleton et al. (2009). All specimens were classified into the 5 toothwear age classes (TWC1–TWC5) defined by Voss (1991; see also Supplementary Data SD3). Four external measurements were recorded: head-body length (HB), tail length (T), hind foot length (HF), and internal length of the ear (E). The 16 craniodental measurements were taken following Musser et al. (1998): occipitonasal length (ONL), greatest zygomatic breadth (ZB),

Downloaded from https://academic.oup.com/jmammal/advance-article-abstract/doi/10.1093/jmammal/gyx149/4697216
by Universidade Federal do Espírito Santo user
on 11 December 2017

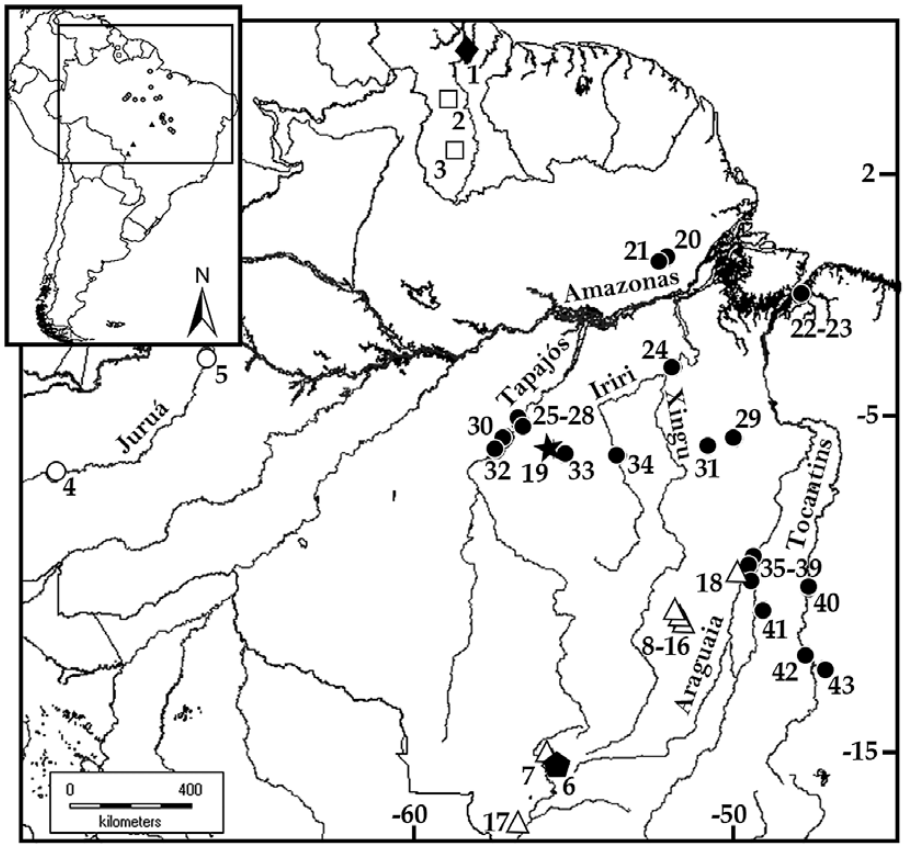

Fig. 1.—Map depicting major river drainages and sampling localities of *Oecomys roberti* (white triangles), *Oecomys tapajinus* (black circles), *Oecomys roberti* from Guyana (white squares), and *Oecomys roberti* from the Juruá River (white circles). Type localities are indicated as a black pentagon for *O. roberti*, black star for *O. tapajinus*, and black diamond for *O. guianae.*

interorbital breadth (IB), rostrum length (LR), rostrum breadth (BR), lambdoidal breadth (LB), braincase height (HBC), zygomatic plate breadth (BZP), diastema length (LD), bony palate length (LBP), breadth of bony palate across first upper molars (BBP), postpalatal length (PPL), incisive foramina length (LIF), incisive foramina breadth (BIF), crown length of maxillary toothrow (CLM1–3), and first upper molar breadth (BM1).

Morphometric analyses were performed using the software PAST 2.14 (Hammer et al. 2001), based on the log-transformed, craniodental measurements of adult specimens (TWC3–TWC5). External measurements were excluded from these analyses because they were either missing from several specimens or they were recorded by different collectors that may have used different measurement conventions. A total of 59 specimens were included in these analyses: 12 *O. roberti*, 40 *O. tapajinus*, and 7 *O. roberti* from Guyana. For each group, we performed descriptive statistical analyses of the craniodental measurements. Data normality was assessed using Shapiro–Wilk's test (Shapiro and Wilk 1965), and only variables with normal distributions were used in subsequent parametric tests. Principal component analysis (PCA) and multivariate analysis of variance (MANOVA) were used to evaluate clusters in morphometric space to verify if they reflected the species identification based on qualitative characters.

Molecular data.—DNA was extracted from liver, muscle, or ear tissue samples preserved in ethanol, using the salt (Bruford et al. 1992) or phenol-chloroform (Sambrook et al. 1989) extraction. We amplified the mitochondrial cytochrome *b* (*Cytb*) and cytochrome *c* oxidase subunit I (*Co1*), and the nuclear intron 7 of the beta fibrinogen (*Fgb*) by polymerase chain reaction (PCR). We used the pair of primers MVZ05 and MVZ16 for *Cytb* (Smith and Patton 1993); a cocktail of primers LepF1_t1, VF1d_t1, LepR1_t1, and VR1d_t1 for *Co1* (Ivanova et al. 2007; modified by E. Eizirik, Pontifícia Universidade Católica do Rio Grande do Sul, pers. comm.); and the pair of primers B17 and βfib (Wickliffe et al. 2003) for *Fgb*. Amplifications were performed using the following PCR profiles: 1) *Cytb*: initial denaturation at 94°C for 5 min, followed by 39 cycles with denaturation at 94°C for 30 s, annealing at 48°C for 45 s, polymerization at 72°C for 45 s, and final extension at 72°C for 5 min; 2) *Co1*: initial denaturation at 94°C for 5 min, followed by 39 cycles with denaturation at 94°C for 30 s, annealing at 60°C for 45 s, polymerization at 72°C for 1 min, and final extension at 72°C for 5 min; 3) *Fgb*: initial denaturation at 94°C for 5 min, followed by 30 cycles with denaturation at 94°C for 30 s, annealing at 56°C for 1 min, polymerization at 72°C for 1 min, and a final extension at 72°C for 7 min. PCR products were purified using ExoSap-IT enzymes (USB Corporation). Mitochondrial fragments were sequenced using an automatic sequencer ABI 3500 (Applied Biosystems, Life Technologies, Thermo Fisher Scientific, Waltham, Massachusetts), using the pairs of primers referenced above for *Cytb* and *Fgb*, and

Downloaded from https://academic.oup.com/jmammal/advance-article-abstract/doi/10.1093/jmammal/gyx149/4697216
by Universidade Federal do Espírito Santo user
on 11 December 2017

the primer M13 for *Co1* (Ivanova et al. 2007; modified by E. Eizirik, Pontifícia Universidade Católica do Rio Grande do Sul, pers. comm.).

Electropherograms were inspected and sequences were aligned using the CLUSTAL W method implemented in MEGA 7 (Kumar et al. 2016). All alignments were inspected and corrected manually. For *Fgb*, heterozygous nucleotide positions were identified by double peaks in the electropherograms, and were coded with International Union of Pure and Applied Chemistry (IUPAC) ambiguity codes. Sequences generated for this study were deposited in GenBank (Supplementary Data SD1). In addition, 5 sequences from species of the *O. roberti* complex and 18 sequences from other species of *Oecomys* were downloaded from the Barcode of Life Data Systems (BOLD) and GenBank (Patton et al. 2000; Borisenko et al. 2008; Rocha et al. 2011a, 2012).

Phylogenetic analyses.—We created a concatenated matrix of *Cytb*, *Co1*, and *Fgb* sequences representing 13 specimens of the *O. roberti* complex (Supplementary Data SD1) using SequenceMatrix (Vaidya et al. 2011). For analyses evaluating *Cytb* and *Co1* separately, we used a total of 32 and 14 sequences, respectively. Additional sequences of other species of *Oecomys* (n = 18) were also included, and *Hylaeamys megacephalus* (Azara's Broad-headed Hylaeamys) and *Euryoryzomys macconnelli* (Macconnell's Euryoryzomys) were used as outgroups.

Phylogenetic relationships among species of *Oecomys* were estimated using Bayesian inference (BI—Lemey et al. 2009) using MrBayes 3.2.5 (Ronquist et al. 2012). BI was performed for the concatenated data and for mitochondrial genes separately. The best model of nucleotide substitution was selected in MrModeltest (Nylander 2004) based on the Akaike Information Criterion (AIC) for each molecular marker (GTR+I+G for *Cytb* and *Co1*, and HKY+I for *Fgb*). Trees were sampled every 500 generations until Markov chain Monte Carlo (MCMC) became stationary, i.e., when *SD* of split frequencies was below 0.01, which is an indicator of good convergence (Lemey et al. 2009). MCMC convergence was also checked in Tracer v.1.6 (Rambaut and Drummond 2013), where we confirmed if effective sample sizes (ESS) were above 200. A 50% majority rule consensus tree was obtained after "burn-in" of 25% of the sample points to generate Bayesian posterior probabilities (BPPs). Consensus trees were visualized in FigTree 1.4 (http://tree.bio.ed.ac.uk/software/figtree/). Genetic distances among clades were estimated using uncorrected (p) distances in MEGA 7 (Kumar et al. 2016). Uncorrected p-distances are preferable for closely related species, and yield higher or comparable identification success than Kimura 2-parameter model (Srivathsan and Meier 2011).

Phylogeography, population structure, and demography.—Phylogeographic relationships, demographic history, and population genetic structure within *O. tapajinus* were explored using only *Cytb* data, which covered a broader geographic range and provided a basic knowledge of putative barriers and geomorphological events (e.g., Leite et al. 2016). Number of haplotypes, polymorphic sites, haplotype and nucleotide diversity values were estimated with DnaSP 5 (Librado and Rozas 2009).

Median-joining (MJ) networks were constructed in NETWORK (Bandelt et al. 1999) using only variable nucleotide sites. Analyses of molecular variance (AMOVAs) among hierarchical groupings of populations were used to depict regional structure using ARLEQUIN 3.5.1.3 (Excoffier and Lischer 2010). We performed AMOVA considering 3 populations from the north bank, south bank, and the mouth of the Amazon River. AMOVAs were performed twice, using haplotype frequencies and accounting for p-distances among haplotypes.

Isolation by distance was assessed using a Mantel test (Mantel 1967). A pairwise geographic distance matrix was obtained in the Geographic Distance Matrix Generator (Ersts 2016). The pairwise genetic distance matrix was obtained by estimating genetic differentiation (F_{ST}) between sampling points, using ARLEQUIN 3.5.1.3 (Excoffier and Lischer 2010). The correlation between genetic and geographic distances was estimated using Isolation by Distance web service 3.23 (Jensen et al. 2005). As geographic distances between sampling localities were heterogeneous, we used a logarithmic transformation ($\log_{10}$) of this matrix to compensate for the disparity among values.

Neutrality and demographic history were evaluated through mismatch distribution and neutrality tests, using DnaSP 5 (Librado and Rozas 2009). Populations under expansion are expected to exhibit smooth and unimodal mismatch distributions, while populations at demographic equilibrium are characterized by ragged and erratic mismatch distributions (Harpending 1994). Deviations from the sudden population expansion model were further tested using the Harpending's raggedness index, which quantify the smoothness of the observed distribution (Harpending 1994). Deviation from neutrality was tested through Tajima's (1989) D, Fu's (1997) Fs, and Ramos-Onsins and Rozas' (2002) R_2 statistics. Coalescence simulations with 1,000 replicates were applied to determine the P-value of each statistics, and significant P-values (< 0.05) were taken as evidence of demographic expansion.

Demographic history was further investigated using Bayesian skyline plots (BSPs) implemented in BEAST 2.1.3 (Bouckaert et al. 2014). We used a strict molecular clock, substitution rates per nucleotide per million year (mean = 0.024, 95% highest posterior density = 0.015–0.035—Leite et al. 2016), and prior best model of nucleotide substitution selected in MrModeltest. We performed two independent runs of 100,000,000 generations each, which were sampled every 10,000 generations. Convergence of the MCMC chains was verified in Tracer v.1.6 by checking the ESS values, and skyline plots were constructed also using Tracer v.1.6 (Rambaut and Drummond 2013).

Results

Morphological and morphometric analyses.—Bivariate plots of the first and the second principal components (PC1 and PC2) showed complete overlap of the 3 groups identified a priori, i.e., *O. roberti* proper, *O. roberti* from Guyana, and *O. tapajinus*. PC1 explained 59.33% of the variation and PC2 explained 12.57% (Fig. 2). For both PC1 and PC2, the measurements that

Downloaded from https://academic.oup.com/jmammal/advance-article-abstract/doi/10.1093/jmammal/gyx149/4697216
by Universidade Federal do Espírito Santo user
on 11 December 2017

contributed most to the variation were zygomatic plate breadth and rostrum breadth. Moreover, all variables contributed positively to PC1, which represents the component related to cranial size. On the other hand, PC2, which is related to cranial shape variation, had both positive and negative variable contributions. In general, *O. roberti* and *O. roberti* from Guyana have intermediate sizes when compared with *O. tapajinus* (Fig. 2; Table 1).

The canonical analyses showed that *O. roberti* and *O. roberti* from Guyana, including their holotypes, are almost completely nonoverlapping (Fig. 2), indicating that they are 2 distinct, well-defined groups in morphometric space, although both overlap with *O. tapajinus*. Indeed, the holotype of *O. tapajinus* is closer to the centroid of *O. roberti* Guyana than to the centroid of *O. tapajinus*. Lambdoidal breadth was the most important measurement on canonical axes 1 and 2 (CA1 and CA2). In addition to substantial morphometric overlap among species of the *O. roberti* complex, qualitative morphological distinction based on cranial and dental characters is also difficult (Fig. 3). This is mainly due to the high level of morphological variation observed in *O. tapajinus*, as documented below under the sections "Morphological description and intraspecific variation," and "Comparisons."

Phylogenetic analyses.—Our phylogenetic analyses recovered 2 distinct and well-supported clades within the *O. roberti* complex (BPP = 1.0), and 2 unsupported clades (Fig. 4). The

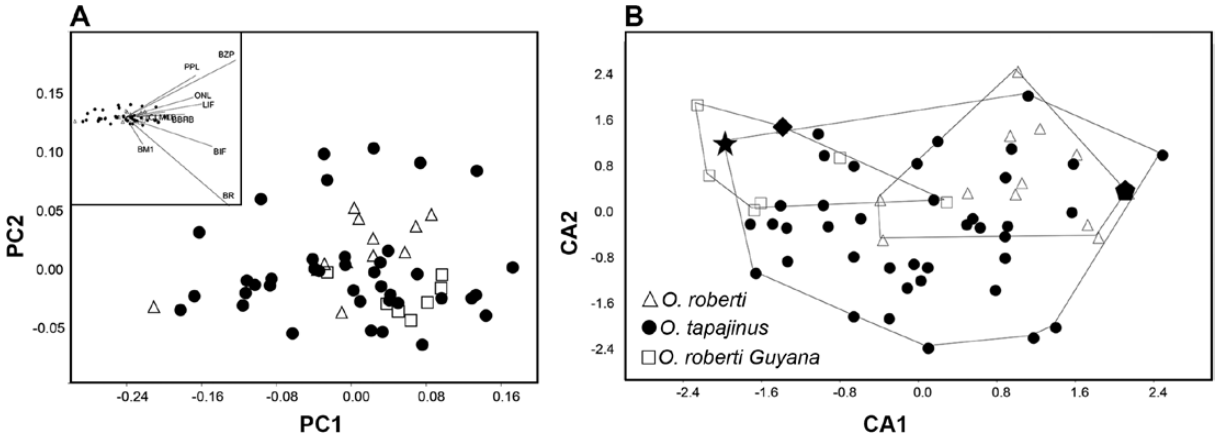

Fig. 2.—Multivariate morphometric analyses of cranial variables of species representing the *Oecomys roberti* complex (n = 59). A) Covariance vectors between the original characters and the first 2 principal component (PC) functions, including projection of individual scores on PC1 × PC2. B) Scores of the 2 principal canonical axes (CA) for each individual. Black star is the holotype of *O. tapajinus*, black diamond is the holotype of *O. guianae*, and black pentagon is the holotype of *O. roberti.* ONL: occipitonasal length; BZP: zygomatic plate breadth; BR: rostrum breadth; IB: interorbital breadth; PPL: postpalatal length; BBP: breadth of bony palate across first upper molars; LIF: incisive foramina length; BIF: incisive foramina breadth; CLM1–3: crown length of maxillary toothrow; BM1: first upper molar breadth.

Table 1.—External, cranial, and dental measurements of holotypes and series of *Oecomys roberti*, *Oecomys tapajinus*, and *Oecomys roberti* Guyana. Mean, *SD*, and range are given in mm. *n* is the sample size. Measurements are defined in "Materials and Methods" section.

Measurement	*O. roberti*				*O. tapajinus*				*O. roberti* Guyana			
	Holotype	Mean ± *SD*	Range	*n*	Holotype	Mean ± *SD*	Range	*n*	Holotype	Mean ± *SD*	Range	*n*
HB	110	112.0 ± 12.98	82.0–130.0	11	126	114.54 ± 13.22	89.0–139.0	35	114			0
T	145	135.73 ± 14.83	101.0–152.0	11	158	134.94 ± 17.29	102.0–171.0	35	149			0
HF	25	25.45 ± 1.57	23.0–28.0	11	25	24.81 ± 1.86	21.0–29.0	35	26	24.8 ± 0.29	24.5–25.0	3
E	16	17.23 ± 0.98	11.0–19.0	11	17	16.66 ± 2.20	10.0–19.0	35	16	14.8 ± 1.04	14.0–16.0	3
ONL	31.91	30.80 ± 1.82	26.41–33.18	10		30.56 ± 2.22	26.69–34.40	37	32.37	31.32 ± 0.71	30.27–32.07	6
ZB	15.99	16.30 ± 1.09	13.58–17.67	11		16.24 ± 1.09	13.85–18.41	38	17.06	16.80 ± 0.65	16.01–17.67	5
IB	5.52	5.50 ± 0.34	4.67–6.03	11	5.8	5.43 ± 0.37	4.49–6.17	39	5.89	5.80 ± 0.29	5.41–6.27	6
LR	8.85	8.45 ± 0.46	7.38–9.23	11	9.79	9.23 ± 1.39	6.77–12.78	38	8.72	8.59 ± 0.24	8.35–8.91	6
BR	5.71	5.38 ± 0.32	4.49–5.64	11	6.6	5.61 ± 0.77	3.70–6.89	39	6.31	6.13 ± 0.27	5.62–6.38	6
LB	12.37	11.98 ± 0.52	10.98–12.48	10		11.73 ± 0.57	10.77–12.96	38	12.11	11.76 ± 0.15	11.55–11.98	6
HBC	9.92	8.80 ± 0.30	8.38–9.22	10		8.97 ± 0.50	7.74–10.64	38	9.55	8.81 ± 0.28	8.37–9.15	6
BZP	3.32	2.99 ± 0.40	2.08–3.48	11	2.93	3.00 ± 0.34	2.38–3.79	39	3.21	3.02 ± 0.11	2.89–3.22	6
LD	8.04	7.93 ± 0.55	6.59–8.53	11	8.99	7.82 ± 0.68	6.49–9.26	39	8.48	8.26 ± 0.29	7.67–8.42	6
LBP	6.4	6.37 ± 0.40	5.55–6.91	11		6.34 ± 0.74	5.24–9.33	39	6.12	6.28 ± 0.22	5.96–6.60	6
PPL	10.92	10.71 ± 0.75	8.96–11.56	10		10.72 ± 0.99	8.43–13.46	34	11.15	10.99 ± 0.52	10.16–11.52	6
BBP	5.71	5.66 ± 0.31	5.11–6.08	11	5.78	5.65 ± 0.30	5.18–6.33	35	5.91	5.82 ± 0.32	5.24–6.12	6
LIF	4.91	4.92 ± 0.27	4.55–5.40	11	5.41	4.87 ± 0.43	4.03–5.81	39	5.53	5.10 ± 0.18	4.88–5.39	6
BIF	2.8	2.56 ± 0.15	2.33–2.87	11	2.97	2.52 ± 0.25	2.06–3.10	39	2.78	2.72 ± 0.21	2.38–2.95	6
CLM1–3	4.99	4.70 ± 0.14	4.47–4.87	11	4.66	4.66 ± 0.23	4.31–5.19	37	4.57	4.67 ± 0.07	4.60–4.74	6
BM1	1.32	1.30 ± 0.08	1.22–1.47	11	1.32	1.29 ± 0.09	1.07–1.56	39	1.35	1.33 ± 0.05	1.28–1.40	6

Downloaded from https://academic.oup.com/jmammal/advance-article-abstract/doi/10.1093/jmammal/gyx149/4697216
by Universidade Federal do Espírito Santo user
on 11 December 2017

Fig. 3.—Dorsal (top) and ventral (bottom) views of the skulls of adult (TWC3) specimens of: A) *Oecomys roberti* (UFMG 2845, female), B) *Oecomys tapajinus* (UFES 1362, male), and C) *Oecomys guianae* (BMNH 10.5.4.27, female), from the collections of the Natural History Museum, London. Scale bar = 5 mm.

name *O. roberti* was given to the least-inclusive clade including the specimen MVZ 197616 (Fig. 4), which is a topotype of *O. roberti*, collected at Chapada dos Guimarães, state of Mato Grosso, Brazil. Similarly, the name *O. tapajinus* was given to the least-inclusive clade including the specimen CAC333 (Fig. 4), which was collected at Moraes Almeida, Itaituba, state of Pará, Brazil, about 40 km south of the type locality of *O. tapajinus* (Santa Rosa, Rio Jamanxim, right bank of the Upper Tapajós, Pará, Brazil—Carleton and Musser 2015). This clade encompasses samples from Tapajós, Xingu, and Araguaia rivers (Figs. 1 and 4). The remaining samples of the *O. roberti* complex formed 2 clades, 1 including specimens from the Juruá River (JLP15241 and JUR542) and the other from Guyana (ROM 98125, 106779, and 111539), but their affinities were uncertain based on concatenated data (Fig. 4). *Oecomys roberti* from Guyana grouped with *O. roberti* proper with high support when only the mitochondrial *Co1* was used (see Supplementary Data SD4 and SD5).

We found high average pairwise genetic distances between *O. roberti* and *O. tapajinus* (*Cytb*: 6.2 ± 0.8%, and *Co1*: 6.9 ± 0.9%; Supplementary Data SD4 and SD5), and low intraspecific genetic distances within them (*Cytb*: 0.4 ± 0.2 and 1.8 ± 0.2, respectively). It should be noted that these 2 species occur in sympatry in the Araguaia River (Fig. 1). Average genetic distances between *O. tapajinus* and *O. roberti* complex specimens from the Juruá River and Guyana are also high (*Cytb*: 6.2 ± 0.7% and *Co1*: 7.2 ± 1.0%, respectively; Supplementary Data SD4 and SD5), but genetic distances between specimens of *O. roberti* proper and *O. roberti* complex from the Juruá and Guiana are slightly lower (*Cytb*: 5.8 ± 0.7% and *Co1*: 4.0 ± 0.7%, respectively; Supplementary Data SD4 and SD5).

Downloaded from https://academic.oup.com/jmammal/advance-article-abstract/doi/10.1093/jmammal/gyx149/4697216
by Universidade Federal do Espírito Santo user
on 11 December 2017

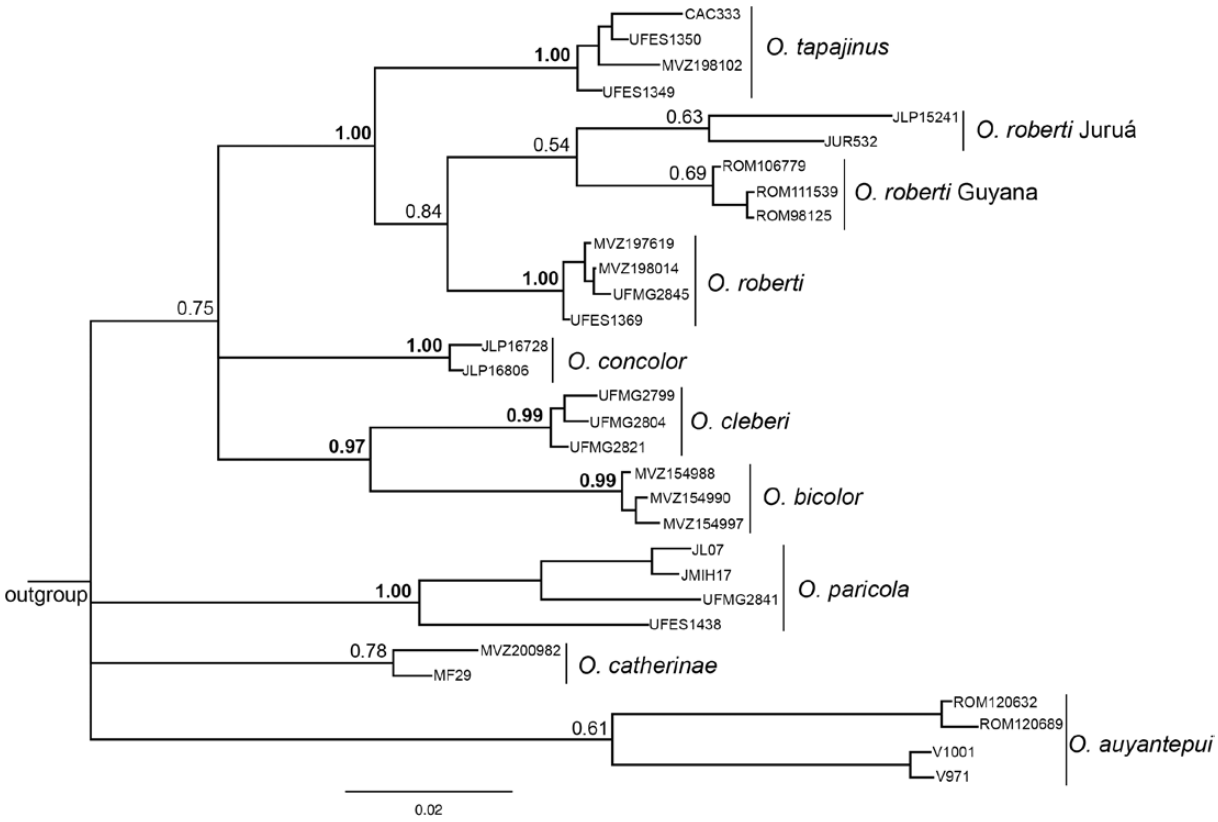

Fig. 4.—Phylogenetic tree of *Oecomys* obtained by Bayesian inference of a concatenated-gene (*Cytb* + *Co1* + *Fgb*) data set. Numbers at nodes are Bayesian posterior probabilities; numbers in bold indicate high support (≥ 0.95). *Hylaeamys megacephalus* and *Euryoryzomys macconnelli* were used as outgroups. Scale bar = 0.02 nucleotide substitutions.

Species delimitation.—Molecular and morphological data are not congruent in delimiting species of the *O. roberti* complex. We choose to follow the phylogenetic results based on molecular data to delimit species of this complex, supporting our hypothesis that *O. tapajinus* is a valid species, distinct from *O. roberti*. Two other groups closely related to *O. tapajinus* and *O. roberti* emerged from our phylogenetic analyses. They are monophyletic based on mitochondrial DNA, but their status as sister clades has low statistical support. Due to the lack of additional data (both molecular and morphological), these groups will continue to be provisionally associated with *O. roberti*. Thus, samples of *O. roberti* from Guyana will be referred to as *O. roberti* Guyana, and samples from the Juruá River will be referred to as *O. roberti* Juruá throughout this paper.

Phylogeography, population structure, and demography.—Our evaluation of partial *Cytb* sequences of 72 individuals of *O. tapajinus* resulted in 28 haplotypes (Supplementary Data SD6), 57 polymorphic sites, high haplotype diversity (0.861 ± 0.035), and low nucleotide diversity (0.009 ± 0.002). MJ networks revealed a star-like configuration, with 2 long branches comprising haplotypes from the north bank of the Amazon River (Amapá) and the mouth of the Amazon River (Belém; Figs. 5 and 6). This structure was corroborated in the *Cytb* BI tree (Supplementary Data SD4).

Analyses of molecular variance revealed differences in the partitioning of genetic variation, depending on the test used (Table 2). When using haplotype frequencies, the majority of variation (59.8%) was found within populations. When using *p*-distances, most variation was found among groups (87.96%). We found no correlation between genetic and geographic distances ($r = 0.0027$, $P = 0.512$), refuting a scenario of isolation by distance. Although mismatch distribution did not show a smooth and unimodal curve ($r = 0.05$, $P = 0.6$; Fig. 6), all neutrality tests ($D = -1.928$, $Fs = -9.666$, and $R_2 = 0.0441$; $P < 0.05$ in each of them) and BSP (Fig. 6) supported scenarios of population expansion.

Taxonomy

Oecomys tapajinus Thomas 1909

Oryzomys [(*Oecomys*)] *tapajinus*: Ellerman 1941:359.

Oryzomys (*Oecomys*) *concolor concolor*: Hershkovitz 1960:546 (part); not *Oecomys concolor* (Wagner 1845).

Oryzomys marmosurus tapajinus: Cabrera 1961:406.

Oecomys trinitatis tapajinus Patterson 1992:25.

Oecomys roberti: Musser and Carleton 1993:716 (part).

Oecomys sp.: Rocha et al. 2011a:19.

Oecomys sp.: Rocha et al. 2011b:711.

Oecomys roberti: Carleton and Musser 2015:408 (part).

Oecomys gr. *roberti*: Rocha et al. 2015:410.

Oecomys aff. *roberti*: Pardiñas et al. 2016:5.

Downloaded from https://academic.oup.com/jmammal/advance-article-abstract/doi/10.1093/jmammal/gyx149/4697216
by Universidade Federal do Espírito Santo user
on 11 December 2017

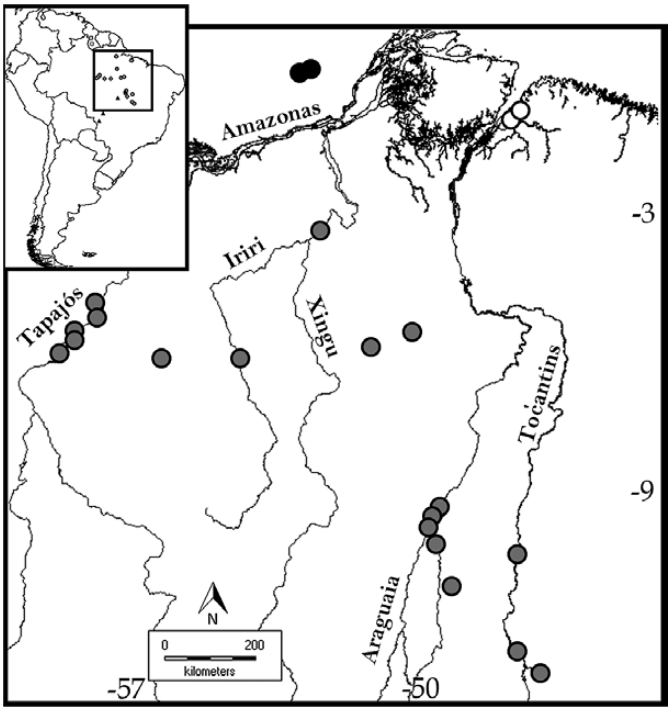

Fig. 5.—Map of sampling localities of the *Oecomys tapajinus* and depicting major river drainages. Colors of sampling localities correspond to those in the median-joining network (Fig. 6A).

Emended diagnosis.—Oecomys tapajinus is characterized by the combination of relatively medium to large size (HB ≈ 89–139 mm, ONL ≈ 26.69–34.40 mm), relatively long tail (TL ≈ 102–171 mm), ventral pelage is gray-based and white-tipped (except chin, throat, inguinal region, and legs, which are pure white or cream, with a midline usually lighter with variable amount of gray), sturdily built skull with well-developed supraorbital ridges that may extend onto parietals, a primitive pattern of carotid circulation represented by a squamosal-alisphenoid groove leading to a sphenofrontal foramen, and anterocone of M1 usually divided by an anteromedian flexus (Supplementary Data SD3).

Geographic distribution.—As reported here, *O. tapajinus* is known from several Brazilian localities in eastern Amazonia and in the transition to the Brazilian Cerrado. It ranges from the mouth of the Amazon River, along the Tocantins, Araguaia, Xingu, Iriri, and Tajapós rivers on the south bank of the Amazon River, as well as the Jari River, on the north bank of the Amazon River (Fig. 1).

Morphological description and intraspecific variation.—Adult HB 89–139 mm (Table 1); TL 104–133% longer than HB (102–171 mm). Dorsal fur soft, 6–11 mm long; adult dorsal pelage tawny, dorsal hairs gray-based and orange-tipped, finely intermixed with completely black guard hairs. Juvenile dorsal pelage dark brownish; older adults brighter than young adults. Head and flanks lighter than dorsum, abrupt lateral transition, well-defined orange line between lateral and ventral fur present in most specimens. Ventral pelage white to cream or gray-based, except chin, throat, inguinal region, and legs totally

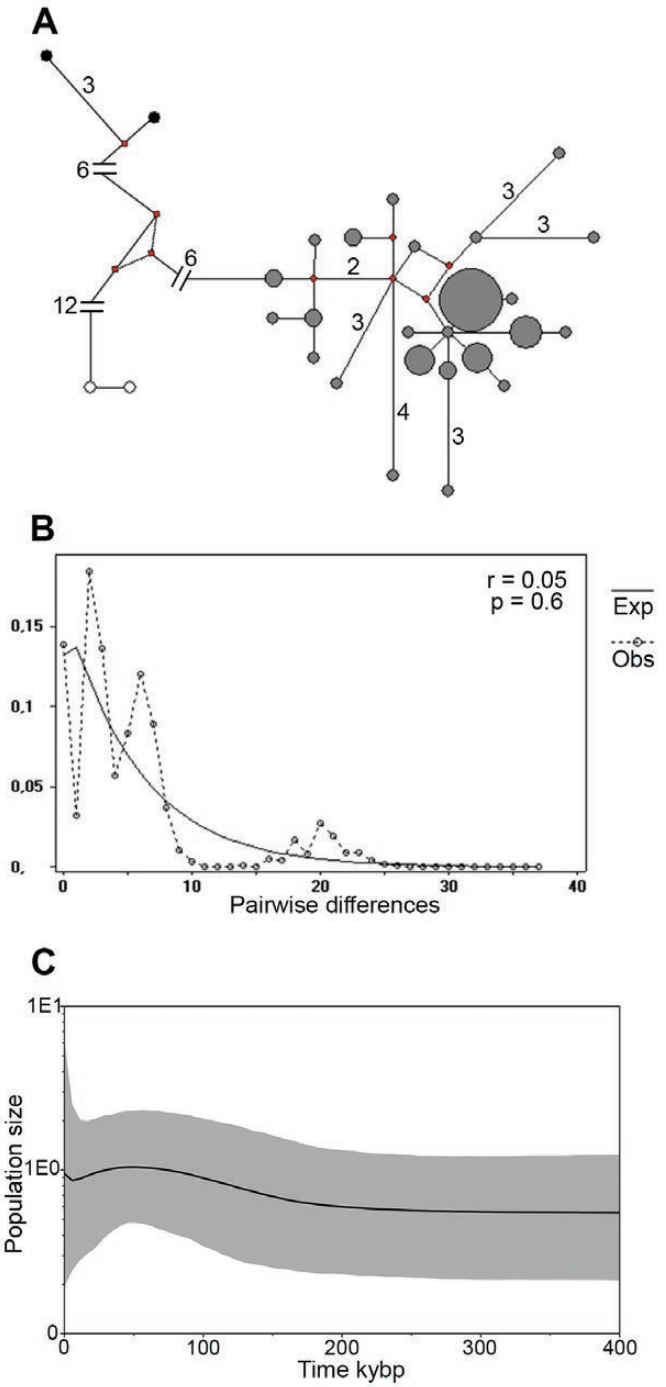

Fig. 6.—Phylogeographic relationships and demographic history of the *Oecomys tapajinus* inferred using *Cytb* sequence data. A) Median-Joining network in which the length of connecting branches corresponds to the nucleotide substitutions, size of the circles is proportional to the number of individuals sharing each haplotype and colors correspond to those in the map (Fig. 5). B) Mismatch distribution in which dashed curves indicate the observed frequency distribution of pairwise differences, and solid curves indicate the distribution that would be expected under a population growth–decline model (θ = 5.203 and τ = 0.198). C) Bayesian skyline plot in which the black solid curve indicates changes in effective population size and gray shadows indicate upper and lower 95% *CI*s.

Downloaded from https://academic.oup.com/jmammal/advance-article-abstract/doi/10.1093/jmammal/gyx149/4697216
by Universidade Federal do Espírito Santo user
on 11 December 2017

Table 2.—Percent variation and fixation indices for the analysis of molecular variance (AMOVA) of *Oecomys tapajinus* considering 3 groups. Numbers in bold correspond to significant values ($P < 0.001$).

	Haplotype frequencies	*p*-distances
% Variation		
Among groups	3.56	87.96
Among pop. within groups	36.63	9.42
Within populations	59.8	2.62
Fixation index		
Φ_{CS}	**0.38**	**0.78**
Φ_{ST}	**0.40**	**0.97**
Φ_{CT}	0.04	**0.88**

white to cream. Some specimens white to cream ventrally with gray-based sides; others gray-based ventrally, except chin and throat, always white to cream. Eyelids black, no eye ring. Mystacial vibrissae black, turning paler toward the tip, and long (32–45 mm), surpassing the ears. Pinnae brown, covered with tiny ochraceous hairs. Hind feet relatively short and broad, dorsal surface partially covered with dark brown-based and white-tipped hairs, general appearance of hind feet dirty white. Ungual tufts bright white and developed on digits II–V. Plantar surface smooth with 6 well-developed pads. Tail completely dark brown, covered with rounded to squared scales, arranged in circles. No caudal pencil, but hairs surpass tail about 1 mm in length. Four pairs of mammae.

Skull sturdy, rostrum short, zygomatic notches shallow. Posterior margins of nasal bones rounded to squared or v-shaped; nasals short or extending a little beyond maxillary-frontal-lacrimal suture. Premaxillary bones about the same level as nasals or a little shorter. Lacrimal contacts both maxillary and frontal. Interorbital region relatively large, convergent anteriorly. Well-developed supraorbital ridges may extend onto parietals; parietals expanded onto lateral surface of the braincase, interparietals expanded laterally. Zygomatic arches wider posteriorly; jugal large, and maxillary and squamosal processes of the zygoma do not overlap. Posterior margin of zygomatic plate anterior to M1 alveolus. Anterior margin of incisive foramina moderately to strongly convergent, and posterior margin almost parallel. Shallow lateral excavations on bony palate. Mesopterygoid fossa broad, U-shaped, reaching the maxillary bones. Posterior palatal pits highly variable, from simple small foramen at each side of the mesopterigoyd fossa, to large and divided foramina, or as divided foramina recessed in a fossa. Parapterygoid fossae dorsally excavated but not reaching the level of the mesopterygoid roof; mesopterygoid roof either totally ossified or with sphenopalatine vacuities anterior to the basisphenoid-presphenoid suture. A primitive pattern of carotid circulation represented by stapedial foramen and posterior opening of alisphenoid canal large, and squamosal-alisphenoid groove and sphenofrontal foramen present; alisphenoid strut usually absent (only 5 out of 34 specimens have this structure on both sides of the skull). Anterior opening of the alisphenoid canal always present as either a small or large foramen. Hamular process of squamosal usually broad, and in most specimens occludes the subsquamosal fenestra, which is a small pit. Ectotympanic bulla small, mastoid either completely ossified or with a diminutive pit in the dorsal contact with the exoccipital border or with a medium-sized fenestra that does not reach the exoccipital border. Mental foramen opens laterally; capsular process of lower incisor present as a slight to medium rounded elevation. Masseteric ridges converge anteriorly as an open bifurcation, below m1, or converge in a single crest.

Upper incisors slightly opisthodont. Labial accessory roots of M1 and m1 present or absent; lingual accessory root of m1 always absent. Maxillary toothrows parallel, 4.31–5.19 mm long. Anteromedian flexus usually present (but absent in the holotype and 9 other specimens) on the anterocone of M1, sometimes diminutive and easily worn with use (Supplementary Data SD3). Anteroloph present on M1 and mesoloph present on M1–2; protoflexus present on M2. Paracone of M1 connected to protocone by enamel bridge situated at posteriormost end of protocone. Accessory loph present on paracone of M2. M3 with mesoloph, posteroloph, and hypoflexus, and smaller than other molars. Anteromedian flexid absent on m1; ectolophid on m1 variable in size, anterolabial cingulum and mesolophids present on m1 and m2, and posteroflexid present on m3.

Comparisons.—Distinction among species of the *O. roberti* complex is difficult due to their morphological similarities (Fig. 3), but the combination of external, cranial, and dental characters allows their identification. All specimens of *O. roberti* examined by us, including the holotype and specimens from the Juruá (Patton et al. 2000), have either a totally white ventral pelage or a white ventral midline from chin to anus, with lateral bands of white-tipped and gray-based fur. Specimens attributable to *O. roberti* Guyana have a spot on the throat without gray-based fur, but the rest of the ventral fur is completely gray-based with cream tips. In contrast, the ventral fur of *O. tapajinus* is white to cream with gray base from chin or neck to anus, although some specimens may exhibit a white ventral midline as described for *O. roberti* proper. Dorsal pelage of specimens attributable to *O. roberti* Guyana, varying from reddish to orangish brown and intermixed with black hairs, is relatively darker than that of both *O. roberti* proper and *O. tapajinus*. Dorsal pelage of specimens of *O. roberti* Juruá is bright reddish orange (Patton et al. 2000). Skulls of *O. roberti* (including those from Guyana) have smaller crests at the interorbital region when compared to *O. tapajinus* and *O. roberti* Juruá, with well-developed crests extending onto the parietals (Patton et al. 2000). The alisphenoid strut is either absent or present in *O. roberti*, *O. roberti* Juruá, and *O. tapajinus*, although always absent in specimens attributable to *O. roberti* Guyana. The anteromedian flexus is absent on M1 of *O. roberti* proper and *O. roberti* Guyana, with rare exceptions (3 out of 25 analyzed specimens have this flexus), but present in *O. tapajinus.* This character was not mentioned for specimens of *O. roberti* from the Juruá (see figure 85 from Patton et al. 2000).

Other congeneric species, such as the White-bellied Oecomys [Oecomys bicolor (Tomes 1860)], the Cleber's Oecomys (*O.*

Downloaded from https://academic.oup.com/jmammal/advance-article-abstract/doi/10.1093/jmammal/gyx149/4697216
by Universidade Federal do Espírito Santo user
on 11 December 2017

cleberi), the Brazilian Oecomys [Oecomys paricola (Thomas 1904)], and the Franciscos's Oecomys Oecomys: (Oecomys franciscorum Pardiñas et al. 2016), have also been documented in eastern Amazonia and in the Amazonia-Cerrado ecotones (Bonvicino et al. 2008; Carleton and Musser 2015), and often occur in sympatry with *O. tapajinus* (e.g., Marinho-Filho et al. 2002; Alho 2005; Rocha et al. 2011a), but they all are easily differentiated from *O. tapajinus* by their size, and skin and skull characteristics (Carleton and Musser 2015; Pardiñas et al. 2016).

Oecomys paricola is easily distinguished from *O. tapajinus* because of its reddish dorsal pelage, totally cream ventral midline from chin to anus flanked by gray-based hairs, and hairy, pencillate tail. Zygomatic notches are shallower and sometimes almost indistinct, interorbital ridges rarely extend onto parietals, and incisive foramina are oval-shaped in *O. paricola.* In addition, the alisphenoid strut is always absent in *O. paricola* (as observed by us and previously mentioned by Voss et al. 2001), and the anteromedian flexus on the anterocone of M1 is absent in *O. paricola*.

Both *O. bicolor* and *O. cleberi* are smaller than *O. tapajinus*, and their dorsal pelage is more yellow. The ventral pelage is pure white in *O. bicolor* and *O. cleberi* has a white to cream midline flanked by gray-based hairs. The tail of both *O. bicolor* and *O. cleberi* ends in a small pencil. In contrast with *O. tapajinus*, these 2 smaller species possess an interorbital region with small crests, very shallow zygomatic notches, elongate incisive foramina, small posterior palatal pits, subsquamosal fenestra always present, and anteromedian flexus on M1 absent.

Compared to *O. tapajinus*, *O. franciscorum* is larger, has a grayish-brown dorsal pelage, and a yellowish midventral pelage flanked by gray-based hairs (Pardiñas et al. 2016). Contrasting with *O. tapajinus*, the interorbital region of *O. franciscorum* is narrow with small crests, the jugal is usually small with overlapping maxillary and squamosal processes, incisive foramina are long and broad medially, and it has a derived carotid circulation pattern, in which the posterior opening of the alisphenoid canal is small, and the squamosal-alisphenoid groove, the sphenofrontal foramen, and the stapedial foramen are all absent.

Discussion

Although provisionally listed as monotypic (Carleton and Musser 2015), cryptic diversity within *O. roberti* has been previously recognized (Rocha et al. 2011a, 2015; Pardiñas et al. 2016). By combining molecular data, including DNA from topotypes of *O. roberti* and *O. tapajinus*, and morphological comparisons of museum specimens, including all type specimens, we were able to confirm Thomas's (1909) view of *O. tapajinus* as a valid species. The recognition of *O. tapajinus* as distinct from *O. roberti* partially reduces the taxonomic intricacies of the *O. roberti* complex, the former being distributed in eastern Amazonia, whereas the latter is known from southern Amazonia. Both species occur in sympatry in the Amazonia-Cerrado ecotone, where their identification in the field is particularly difficult (Rocha et al. 2011a, 2015).

Oecomys tapajinus and *O. roberti* are phenetically very similar, mainly due to the high morphological variation reported for *O. tapajinus*, but these 2 species represent 2 reciprocally monophyletic and genetically distant entities (*Cytb*: 6.2 ± 0.8%, and *Co1*: 6.9 ± 0.9%) that occur in sympatry, indicating that they represent separate lineages that merit species-level status. However, a few qualitative morphological characters are useful in distinguishing these 2 species, including predominately gray-based ventral fur (totally white ventral pelage or a white ventral midline from chin to anus, with lateral bands of white-tipped and gray-based fur in *O. roberti*), a more heavily built skull with longer interorbital ridges (smaller interorbital crests in *O. roberti*), and anteromedian flexus present on M1 in *O. tapajinus* (absent in *O. roberti*). This last character is uncommon in *Oecomys* (Weksler 2006), and was previously considered a discriminating feature between *Oecomys* and *Rhipidomys* (as observed by us and by M. D. Carleton, National Museum of Natural History, Smithsonian Institution, pers. comm.). Further morphological discrimination between *O. tapajinus* and *O. roberti* will depend on the analyses of additional series of specimens, especially from the latter.

Two other groups closely related to *O. tapajinus* and *O. roberti* emerged from our phylogenetic analyses, 1 including specimens from the Juruá River (*O. roberti* Juruá) and the other from Guyana (*O. roberti* Guyana). Although both were recovered as monophyletic based on mitochondrial DNA, their status as sister clades had low statistical support. The genetic distances between them and *O. roberti* are lower (5.8% and 4.0%, respectively) than those reported as indicative of distinct species of *Oecomys* (7–10%—Pardiñas et al. 2016), but not different from the distances between *O. roberti* and *O. tapajinus* reported here. Patton et al. (2000) identified specimens from the Juruá River as *O. roberti* because their morphology matches the description of this species and their close genetic distance to the topotype of *O. roberti* confirms this identification (Fig. 4). Samples of *O. roberti* Guyana may be associated to the synonym *O. guianae*, due to the geographic provenance of the specimens. *Oecomys guianae* is still considered a junior synonym of *O. roberti*, but it should be noted that specimens separated into 2 different and well-defined clusters in morphometric space (Fig. 2), and some morphologically distinct characters were recorded in *O. roberti* Guyana, including darker dorsal pelage, ventral pelage with a spot in the throat without gray-based fur, being the rest of the ventral fur completely gray-based with cream tips, a more delicate skull and alisphenoid strut always absent. Further study using morphological and molecular data from specimens collected throughout the wide range of *O. roberti* may shed light on the taxonomic status of its synonym *O. guianae*, which may also represent a valid species.

Our phylogeographic analyses revealed 3 main haplogroups within *O. tapajinus* located to the north, south, and at the mouth of the Amazon River. This result was corroborated by high genetic differentiation among these 3 groups, found in analyses

Downloaded from https://academic.oup.com/jmammal/advance-article-abstract/doi/10.1093/jmammal/gyx149/4697216
by Universidade Federal do Espírito Santo user
on 11 December 2017

of molecular variance. Moreover, we found no correlation between genetic and geographic distances, refuting a scenario of isolation by distance. Therefore, genetic divergence and structure seem to be related with landscape features, specifically with the complex system of the Amazon River. No evidence of riverine barrier effects on this species was detected in a previous study (Rocha et al. 2014), which suggests that this species uses forested river islands as stepping stones facilitating gene flow between river banks. However, our results indicate that the Amazon River seems to constitute a stronger barrier to the gene flow of this small mammal species, probably due to its wider width when compared to the Araguaia River. Additional demographic analyses supported a scenario of population expansion, which may be related to forest expansions during glaciations. *Oecomys tapajinus* is an arboreal, forest specialist species and prefers flooded forests (Ramos Pereira et al. 2013; Rocha et al. 2014). Thus, it is expected that population dynamics have followed forest expansion or retraction in the past (e.g., Cabanne et al. 2016; Leite et al. 2016). Our explanation is corroborated by palynological and climatological studies indicating expansions of humid forest into open biomes during glaciations (Ledru et al. 1998; Ledru 2002).

In summary, we show that analyses of morphological and molecular variation through space are essential in the identification of cryptic species such as those belonging to the genus *Oecomys*. Here, we confirm the taxonomic status of *O. tapajinus* as a valid species, and provide evidence that the junior synonym *O. guianae* may also represent a separate taxonomic unit from *O. roberti*. When allied to ecological data, this knowledge enhances our understanding of the processes behind species diversification and coexistence in megadiverse regions such as the Neotropics.

Supplementary Data

Supplementary data are available at *Journal of Mammalogy* online.

Supplementary Data SD1.—Morphological and molecular data used in this study.

Supplementary Data SD2.—Gazetteer.

Supplementary Data SD3.—Maxillary and mandibular molars of *Oecomys tapajinus* of each toothwear age class.

Supplementary Data SD4.—Phylogeny of *Oecomys* obtained by Bayesian inference of a cytochrome *b* gene data set.

Supplementary Data SD5.—Phylogeny of *Oecomys* obtained by Bayesian inference of a cytochrome *c* oxidase subunit I gene data set.

Supplementary Data SD6.—List of the cytochrome *b* haplotypes of *Oecomys tapajinus*, with their frequencies and specimens.

Acknowledgments

We are very grateful to the following curators and collection support staffs for making specimens available: P. Jenkins, L. Tomsett, and R. Portela (BMNH), S. Marques-Aguiar (MPEG), M. de Vivo (MZUSP), J. Dalapicolla and M. Nascimento (UFES), A. Paglia and F. Perini (UFMG). We also thank J. Patton who kindly shared nucleotide sequences generated from previous studies, J. Justino (UFES) who provided laboratory assistance, and C. Azevedo (UFES) for nomenclatural advice. We thank the Natural History Museum, London, for the permission to use the image of *Oecomys guianae* from their collections. RGR had a research grant from *Fundação de Amparo a Pesquisa e Inovação do Espírito Santo*, Brazil (FAPES, ref.: 0650.2015). LPC and YLRL had support from *Conselho Nacional de Desenvolvimento Científico e Tecnológico*, Brazil (CNPq, refs.: 307214.2015-0 and 305008.2013-7, respectively) and FAPES (ref.: 61864315). We thank D. Rogers and 2 anonymous reviewers for their valuable comments on a previous version of this manuscript.

Literature Cited

Alho, C. J. R. 2005. Intergradation of habitats of non-volant small mammals in the patchy Cerrado landscape. Arquivos do Museu Nacional, Rio de Janeiro 63:41–48.

Bandelt, H. J., P. Forster, and A. Röhl. 1999. Median-joining networks for inferring intraspecific phylogenies. Molecular Biology and Evolution 16:37–48.

Bickford, D., et al. 2006. Cryptic species as a window on diversity and conservation. Trends in Ecology & Evolution 22:148–155.

Bonvicino, C. R., J. A. Oliveira, and P. S. D'Andrea. 2008. Guia dos roedores do Brasil, com chaves para géneros baseadas em caracteres externos. Centro Pan-Americano de Febre Aftosa, Rio de Janeiro, Brazil.

Borisenko, A. V., B. K. Lim, N. V. Ivanova, R. H. Hanner, and P. D. Hebert. 2008. DNA barcoding in surveys of small mammal communities: a field study in suriname. Molecular Ecology Resources 8:471–479.

Bouckaert, R., et al. 2014. BEAST 2: a software platform for Bayesian evolutionary analysis. PLoS Computational Biology 10:e1003537.

Bruford, M., O. Hanotte, J. Brookfield, and T. Burke. 1992. Single-locus and DNA fingerprinting. Pp. 225–269 in Molecular genetic analyses of populations. A pratical approach (A. Hoelzel, ed.). IRL Press, Oxford, United Kingdom.

Cabanne, G. S., et al. 2016. Effects of Pleistocene climate changes on species ranges and evolutionary processes in the Neotropical Atlantic. Biological Journal of the Linnean Society 119:856–872.

Cabrera, A. 1961. Catálogo de los mamíferos de América del Sur. Revista del Museo Argentino de Ciencias Naturales 4:309–732.

Carleton, M. D., L. H. Emmons, and G. G. Musser. 2009. A new species of the rodent genus *Oecomys* (Cricetidae: Sigmodontinae: Oryzomyini) from Eastern Bolivia, with emended definitions of *O. concolor* (Wagner) and *O. mamorae* (Thomas). American Museum Novitates 3661:1–32.

Carleton, M. D., and G. G. Musser. 2015. Genus *Oecomys* Thomas, 1906. Pp. 393–417 in Mammals of South America, volume 2. Rodents (J. L. Patton, U. F. J. Pardiñas, and G. D'Elia, eds.). University of Chicago Press, Chicago, Illinois.

Chakrabarty, P. 2010. Genetypes: a concept to help integrate molecular phylogenetics and taxonomy. Zootaxa 2632:67–68.

Ellerman, J. R. 1941. The families and genera of living rodents. Trustees of the British Museum, London, United Kingdom.

Downloaded from https://academic.oup.com/jmammal/advance-article-abstract/doi/10.1093/jmammal/gyx149/4697216
by Universidade Federal do Espírito Santo user
on 11 December 2017

Ersts, P. J. 2016. Geographic Distance Matrix Generator (version 1.2.3). American Museum of Natural History, Center for Biodiversity and Conservation. http://biodiversityinformatics.amnh.org/open_source/gdmg. Accessed 7 August 2017.

Excoffier, L., and H. E. Lischer. 2010. Arlequin suite ver 3.5: a new series of programs to perform population genetics analyses under Linux and Windows. Molecular Ecology Resources 10:564–567.

Fu, Y. X. 1997. Statistical tests of neutrality of mutations against population growth, hitchhiking and background selection. Genetics 147:915–925.

Hammer, Ø., D. A. T. Harper, and P. D. Ryan. 2001. PAST: paleontological statistics software package for education and data analysis. Palaeontologia Electronica 4:1–9.

Harpending, H. C. 1994. Signature of ancient population growth in a low-resolution mitochondrial DNA mismatch distribution. Human Biology 66:591–600.

Hershkovitz, P. 1960. Mammals of the northern Colombia, preliminary report nº 8: arboreal rice rats, a systematic revision of the sub-genus *Oecomys*, genus *Oryzomys*. Proceedings of US National Museum 110:513–568.

Ivanova, N. V., T. S. Zemlak, R. H. Hanner, and P. D. Hebert. 2007. Universal primer cocktails for fish DNA barcoding. Molecular Ecology Notes 7:544–548.

Jensen, J. L., A. J. Bohonak, and S. T. Kelley. 2005. Isolation by distance, web service. BMC Genetics 6:13.

Kumar, S., G. Stecher, and K. Tamura. 2016. MEGA7: molecular evolutionary genetics analysis version 7.0 for bigger datasets. Molecular Biology and Evolution 33:1870–1874.

Ledru, M. 2002. Late Quaternary history and evolution of the cerrados as revealed by palynological records. Pp. 33–49 in The cerrados of Brazil: ecology and natural history of a Neotropical savanna (P. Oliveira and R. Marquis, eds.). Columbia Uniersity Press, New York City, New York.

Ledru, M. P., L. Salgado-Labouriau, and L. Lorscheitter. 1998. Vegetation dynamics in southern and central Brazil during the last 10,000 yr B. P. R. Review of Palaeobotany and Palynology 99:131–142.

Leite, Y. L. R., et al. 2016. Neotropical forest expansion during the last glacial period challenges refuge hypothesis. Proceedings of the National Academy of Sciences of the United States of America 113:1008–1013.

Lemey, P., M. Salemi, and A.-M. Vandamme (eds.). 2009. The phylogenetic handbook: a practical approach to phylogenetic analysis and hypothesis testing. 2nd ed. Cambridge University Press, Cambridge.

Librado, P., and J. Rozas. 2009. DnaSP v5: a software for comprehensive analysis of DNA polymorphism data. Bioinformatics 25:1451–1452.

Locks, M. 1981. Nova espécie de *Oecomys* de Brasília, DF, Brasil (Cricetidae, Rodentia). Boletim do Museu Nacional 300:1–7.

Mantel, N. 1967. The detection of disease clustering and a generalized regression approach. Cancer Research 27:209–220.

Marinho-Filho, J., F. H. G. Rodrigues, and K. M. Juarez. 2002. The Cerrado mammals: diversity, ecology, and natural history. Pp. 266–284 in The Cerrados of Brazil, ecology and natural history of a Neotropical savanna (P. A. Oliveira and R. J. Marquis, eds.). Columbia University Press, New York City, New York.

Musser, G. G., and M. D. Carleton. 1993. Family Muridae. Pp. 501–755 in Mammal species of the world (D. E. Wilson and D. M. Reeder, eds.). 2nd ed. Smithsonian Institution Press, Washington, D.C.

Musser, G. G., M. D. Carleton, E. M. Brothers, and A. L. Gardner. 1998. Systematic studies of Oryzomyine rodents (Muridae, Sigmodontinae): diagnoses and distributions of species formerly assigned to *Oryzomys "capito"*. Bulletin of the American Museum of Natural History 236:1–376.

Nylander, J. A. A. 2004. MrModeltest, version 2. Program distributed by the author. Evolutionary Biology Centre, Uppsala University, Uppsala, Sweden. https://github.com/nylander/MrModeltest2. Accessed 7 August 2017.

Pardiñas, U. F. J., P. Teta, J. Salazar-Bravo, P. Myers, and C. A. Galliari. 2016. A new species of arboreal rat, genus *Oecomys* (Rodentia, Cricetidae) from Chaco. Journal of Mammalogy 97:1177–1196.

Patterson, B. D. 1992. Mammals in the Royal Natural History Museum, Stockholm, collected in Brazil and Bolivia by A. M. Olalla during 1934–1938. Fieldiana Zoologia, New Series 66:1–42.

Patton, J. L., M. Nazareth, F. D. A. Silva, and J. A. Y. R. Malcolm. 2000. Mammals of the Rio Juruá and the evolutionary and ecological diversification of Amazonia. Bulletin of the American Museum of Natural History 244:1–306.

Rambaut, A., and A. J. Drummond. 2013. Tracer. University of Edinburgh, Edinburgh, United Kingdom. beast.bio.ed.ac.uk/Tracer. Accessed 7 August 2017.

Ramos-Onsins, S. E., and J. Rozas. 2002. Statistical properties of new neutrality tests against population growth. Molecular Biology and Evolution 19:2092–2100.

Ramos Pereira, M., R. G. Rocha, E. Ferreira, and C. Fonseca. 2013. Structure of small mammal assemblages across flooded and unflooded gallery forests of the Amazonia-Cerrado ecotone. Biotropica 45:489–496.

Rocha, R. G., et al. 2011a. Small mammals of the mid-Araguaia River in central Brazil, with the description of a new species of climbing rat. Zootaxa 34:1–34.

Rocha, R. G., E. Ferreira, C. Fonseca, J. Justino, Y. L. Leite, and L. P. Costa. 2014. Seasonal flooding regime and ecological traits influence genetic structure of two small rodents. Ecology and Evolution 4:4598–4608.

Rocha, R. G., E. Ferreira, Y. L. R. Leite, C. Fonseca, and L. P. Costa. 2011b. Small mammals in the diet of Barn owls, *Tyto alba* (Aves: Strigiformes) along the mid-Araguaia River in central Brazil. Zoologia 28:709–716.

Rocha, R. G., C. Fonseca, Z. Zhou, Y. L. R. Leite, and L. P. Costa. 2012. Taxonomic and conservation status of the elusive *Oecomys cleberi* (Rodentia, Sigmodontinae) from central Brazil. Mammalian Biology 77:414–419.

Rocha, R. G., J. Justino, Y. L. R. Leite, and L. P. Costa. 2015. DNA from owl pellet bones uncovers hidden biodiversity. Systematics and Biodiversity 13:403–412.

Ronquist, F., et al. 2012. Efficient Bayesian phylogenetic inference and model choice across a large model space. Systematic Biology 61:539–542.

Rosa, C. C., et al. 2012. Genetic and morphological variability in South American rodent *Oecomys* (Sigmodontinae, Rodentia): evidence for a complex of species. Journal of Genetics 91:265–277.

Sambrook, J., E. F. Fritschi, and T. Maniatis. 1989. Molecular cloning: a laboratory manual. Cold Spring Harbor Laboratory Press, New York.

Shapiro, S. S., and M. B. Wilk. 1965. An analysis of variance test for normality (complete samples). Biometrika 52:591–611.

Sikes, R. S., and The Animal Care and Use Committee of the American Society of Mammalogists. 2016. Guidelines of the American Society of Mammalogists for the use of wild mammals in research and education. Journal of Mammalogy 97:663–688.

Downloaded from https://academic.oup.com/jmammal/advance-article-abstract/doi/10.1093/jmammal/gyx149/4697216
by Universidade Federal do Espírito Santo user
on 11 December 2017

SMITH, M. F., AND J. L. PATTON. 1993. The diversification of South American murid rodents: evidence from mitochondrial DNA sequence data for the akodontine tribe. Biological Journal of the Linnean Society 50:149–177.

SMITH, M. F., AND J. L. PATTON. 1999. Phylogenetic relationships and the radiation of Sigmodontine rodents in South America: evidence from cytochrome b. Journal of Mammalian Evolution 6:89–128.

SRIVATHSAN, A., AND R. MEIER. 2011. On the inappropriate use of Kimura-2-parameter (K2P) divergences in the DNA-barcoding literature. Cladistics 28:190–194.

TAJIMA, F. 1989. Statistical method for testing the neutral mutation hypothesis by DNA polymorphism. Genetics 123:585–595.

THOMAS, O. 1904. New Callithrix, Midas, Felis, *Rhipidomys* and *Proechimys* from Brazil and Ecuador. Annals and Magazine of Natural History, Series 7, 14:188–196.

THOMAS, O. 1906. Notes on South American rodents II. On the allocation of certain species hitherto referred respectively to *Oryzomys*, *Thomasomys* and *Rhipidomys*. Annals and Magazine of Natural History 7:442–445.

THOMAS, O. 1909. New species of *Oecomys* and *Marmosa* from Amazonia. The Annals and Magazine of Natural History 3:378–380.

THOMAS, O. 1910. Mammals from the River Supinaam, Demerara, presented by Mr. F. V. McConnell to the British Museum. Annals and Magazine of Natural History: Series 8 7:606–608.

TOMES, R. F. 1860. Notes on a second collection of Mammalia made by Mr. Fraser in the Republic of Ecuador. Proceedings of Zoological Society of London 1860:211–221.

VAIDYA, G., D. J. LOHMAN, AND R. MEIER. 2011. SequenceMatrix: concatenation software for the fast assembly of multi-gene datasets with character set and codon information. Cladistics 26:171–180.

VOSS, R. S. 1991 An introduction to the Neotropical muroid rodent genus *Zygodontomys*. Bulletin of the American Museum of Natural History 210:1–113.

VOSS, R. S., D. P. LUNDE, AND N. B. SIMMONS. 2001. The mammals of Paracou, French Guiana: a Neotropical lowland rainforest fauna part 2. Nonvolant species. Bulletin of the American Museum of Natural History 263:1–235.

WAGNER, J. A. 1845. Diagnosen einiger neuen Arten von Nager und Handflulern. Arch Naturgeschichte 11:145–149.

WEKSLER, M. 2003. Phylogeny of Neotropical Oryzomyine rodents (Muridae: Sigmodontinae) based on the nuclear IRBP exon. Molecular Phylogenetics and Evolution 29:331–349.

WEKSLER, M. 2006. Phylogenetic relationships of Oryzomine rodents (Muroidea: Sigmodontinae): separate and combined analyses of morphological and molecular data. Bulletin of the American Museum of Natural History 296:1–149.

WICKLIFFE, J. K., F. G. HOFFMANN, D. S. CARROLL, Y. V. DUNINA-BARKOVSKAYA, R. D. BRADLEY, AND R. J. BAKER. 2003. Intron 7 (FGB-17) of the fibrinogen, B beta polypeptide (FGB): a nuclear DNA phylogenetic markers for mammals. Occasional Papers, Museum of Texas Tech University 219:1–6.

Submitted 10 October 2016. Accepted 18 October 2017.

Associate Editor was Duke Rogers.

Downloaded from https://academic.oup.com/jmammal/advance-article-abstract/doi/10.1093/jmammal/gyx149/4697216
by Universidade Federal do Espírito Santo user
on 11 December 2017
View publication stats